

Cite this: *Polym. Chem.*, 2024, **15**, 3327

# Insights into hydrophobic (meth)acrylate polymers as coating for slow-release fertilizers to reduce nutrient leaching†

Asma Sofyane,<sup>a</sup> Salima Atlas,<sup>a,b</sup> Mohammed Lahcini,<sup>a,c</sup> Elvira Vidović,<sup>d</sup> Bruno Ameduri<sup>\*e</sup> and Mustapha Raihane<sup>\*a,f</sup>

To solve the problem of the low utilization rate of conventional fast-release water-soluble fertilizers and to minimize their negative impact on the environment, slow-release fertilizers (SRFs) have emerged as a sustainable solution to limit their losses, reduce fertilizer dosage and improve crop production. In this study, new hydrophobic (meth)acrylate polymers (poly(2,2,2-trifluoroethyl methacrylate) (PTFEMA) and poly(2-(perfluorohexyl)ethyl acrylate) (PPFEHEMA)) with different fluorinated side chains were synthesized by free radical polymerization and used as coatings for SFRs. These polymers were characterized by <sup>1</sup>H and <sup>19</sup>F NMR, FTIR, WCA, TGA and DSC. Compared to PTFEMA, PPFEHEMA with a higher content of F atoms displayed improved thermal stability and an elastomer property ( $T_g = -10$  °C) leading to satisfactory film formation. Indeed, water contact angle (WCA) measurements were carried out on films of both materials: PPFEHEMA with WCA = 109° indicated a highly hydrophobic character with an excellent water-repellent surface, resulting in a coating layer. The use of these polymers as SFR coatings was explored using dip-coating. SEM and EDX mapping were performed to study the morphology of the coated fertilizer granules and showed the formation of a cohesive film with good adhesion between the DAP fertilizer and the coating films, limiting water diffusion. The release profiles of N and P nutrients were studied, and the corresponding release times increased with coating thickness (single layer: 1L or second layer: 2L). Compared to uncoated DAP granules which are totally solubilized after less than 2 h, DAP coated with 2L of PPFEHEMA shows the slowest release of N and P nutrients, and the times to reach maximum N and P releases were 30 and 38 times higher than those of uncoated DAP. The significant delay in the release of nutrients from DAP coated with PTFEMA or PPFEHEMA is consistent with nutrient demand during crop growth and increases the efficiency of fertilizer use and therefore enhances agricultural productivity.

Received 24th May 2024,  
Accepted 15th July 2024

DOI: 10.1039/d4py00573b

rsc.li/polymers

## 1. Introduction

From the data of the population projections published by the United Nations, the world population will reach 9.5 billion

people by 2050,<sup>1</sup> with a planned increase in food supply of 70%.<sup>2</sup> The forecast of the Food and Agriculture Organization of the United Nations (FAO) estimates that a quarter of this growing population could suffer from food insecurity. Around 30% of arable land will be lost due to soil degradation.<sup>3</sup> In order to meet the growing global demand for food and to address food security challenges by promoting sustainable agriculture, the use of inorganic nitrogen (N), phosphorus (P) and potassium (K) fertilizers is expected to increase because they can improve crop productivity by about 60%.<sup>4</sup> However, current conventional fertilizers are highly water-soluble, meaning that only 30–60% of N, 10–20% of P and 30–50% of K could be absorbed by plants. A large amount of these micronutrients is released into the environment through leaching, runoff, volatilization, etc., which has a negative impact on ecosystems and biodiversity, such as soil disturbance and ground-water contamination. These losses result not only in low absorption efficiency of the nutrients by plant roots,<sup>5</sup> but also

<sup>a</sup>IMED-Lab. Faculty of Sciences and Techniques, Cadi-Ayyad University, Av. A. Khattabi. BP 549, 40000 Marrakech, Morocco. E-mail: m.raihane@uca.ma

<sup>b</sup>ERSIC, FPBM, Sultan Moulay Slimane University, PO. Box. 592, Mghila, 23000, Beni Mellal, Morocco

<sup>c</sup>Mohammed VI Polytechnic University, 43150 Ben Guérir, Morocco

<sup>d</sup>Faculty of Chemical Engineering and Technology, University of Zagreb, Marulićev trg 19, 10000 Zagreb, Croatia

<sup>e</sup>ICGM, University of Montpellier, CNRS, ENSCM, 34095 Montpellier, France. E-mail: bruno.ameduri@enscm.fr

<sup>f</sup>Applied Chemistry and Engineering Research Centre of Excellence (ACER CoE), Mohammed VI Polytechnic University, Lot 660, Hay Moulay Rachid Ben Guérir, 43150, Morocco

† Electronic supplementary information (ESI) available. See DOI: <https://doi.org/10.1039/d4py00573b>



in financial losses due to the waste of energy associated with their production.<sup>6,7</sup> Therefore, in order to maximize crop production one of the major challenges is to rationalize the use of fertilizers. Slow-release fertilizers (SRFs) are proposed as a promising technology to improve nutrient uptake by plants and to minimize environmental pollution.<sup>8</sup> SRFs are designed to release nutrients slowly to meet their needs during crop growth.<sup>9</sup> Polymers coated fertilizers are the most important candidates for SRFs because the polymer acts as a diffusion barrier membrane. Polyolefin, alkyd-resin and polyurethane-coated fertilizers are important commercially available synthetic polymer coatings for SRFs, manufactured by JCAM AGRI Co, ICL Specialty Fertilizers and Koch Agronomic Services, Inc. under the Nutricote®, Osmocote® and Polyon® trademarks<sup>10</sup> (more details are given in ESI†). The synthetic polymer coatings can be divided into two classes: (i) hydrophobic polyolefins which are soluble in an organic solvent (*e.g.*, polyethylene<sup>11</sup> or polyacrylonitrile<sup>12</sup>), and (ii) superabsorbent hydrogels as three-dimensional or crosslinked matrices composed of linear or branched polymers with abundant hydrophilic groups,<sup>13</sup> which in agriculture lead to increased water storage capacity, a limited amount of irrigation, and increased crop production in semi-arid and arid areas.<sup>14</sup>

Poly(acrylate)s (PAs) have been widely used to produce SRFs to increase agricultural yields of corn and wheat<sup>15</sup> and as superabsorbents.<sup>16</sup> PA waterborne coatings using an aqueous solution in their preparation are known for their appropriate viscosity, good film-forming ability, and strong adhesion to substrates through polar groups.<sup>17</sup> Polysaccharides such as starch or cellulose are used as biopolymers for the synthesis of bio-superabsorbents in which vinyl monomers such as methacrylic acid, acrylamide, or acrylic acid are grafted onto their backbones to increase the hydrophilicity and swelling capacity of these superabsorbents.<sup>18</sup> To elaborate these networks to give them enhanced water-retention capacity and regulated slow-release of nutrients, grafting reactions have been performed in an aqueous solution by free radical (co) polymerization of these monomers using ammonium persulfate and *N,N'*-methylenebisacrylate (MBA) as initiator and crosslinking agent, respectively.<sup>16</sup> Recently, Zhu *et al.*<sup>19</sup> prepared superabsorbent hydrogel composites based on okara, a byproduct derived from soybean oil milk, grafted onto poly(acrylic acid), by *in situ* radical polymerization to improve vegetable cultivation through increasing the water holding capacity in soils. Jumpapaeng *et al.*<sup>20</sup> prepared bionanocomposite hydrogels (BHMs) as a promising material by combining cassava starch, polyacrylamide, natural rubber, and various montmorillonite clay loadings. These low-cost biohydrogels exhibit high-strength properties and serve as coating membranes for slow-release urea fertilizers. However, these hydrogels present some defect pores when used as a coating on the surface of urea, increasing the solubility of the N nutrient and thus reducing the slow-release effect. To address this issue, a wax hydrophobic polymer solution was used to encapsulate the BHM hydrogel surfaces as an outer layer by filling in all cracks and defects detected on the surface. These hydrophobic

and continuous wax layers improve the structural stability of the coating materials and enhance the slow-release performance by preventing water penetration into the fertilizer core.

With the above problems in the use of hydrophilic superabsorbent polymers, hence hydrophobic polymer coating films present an answer to this challenge by acting as good barrier membranes to limit the diffusion of water, and thus delay nutrient release from coated fertilizers. Among these polymers, fluorinated acrylate polymers are the most commonly proposed materials thanks to their remarkable properties, such as UV photo-chemical stability, remarkable weatherability, semi-permeable membranes, and self-cleaning surfaces.<sup>21–23</sup> Homo- and copolymers of fluorinated (meth)acrylates with perfluoroalkyl side chains ( $C_nF_{2n+1}$ ) are an important class of such materials that exhibit unexpected hydrophobicity in comparison to the corresponding *n*-alkyl chains (PAs). In fact, the fluorocarbons side chains pack less densely on the surfaces, leading to poorer van der Waals interactions with water and thus to good water-repellent properties.<sup>21,24–26</sup> Their low surface energies, attributed to the properties of fluorine atoms, enable them to be widely used in high-performance coatings.<sup>25–29</sup>

To our knowledge, there have been only two papers reporting the use of hydrophobic fluorinated polymers as SRF coatings. To enhance the performance of polymer-encapsulated urea fertilizers, Chen *et al.*<sup>30</sup> developed a novel waterborne hydrophobic polymer coating using nano-SiO<sub>2</sub> and 1*H*,1*H*,2*H*,2*H*-perfluorooctyltriethoxysilane to modify water-based polyvinyl alcohol. More recently waterborne copolymers prepared by Pickering emulsion copolymerization of butyl methacrylate (BMA) with 2-(perfluorohexyl)ethyl acrylate (PFEHEMA) were reported by our team. The resulting waterborne latexes were tested as coating materials for granular water-soluble fast-release fertilizers.<sup>31</sup> A P(BMA-*co*-PFEHEMA) copolymer containing 8 wt% starch nanocrystals and a low PFEHEMA percentage (6.5 mol%) showed better slow-release properties than those of non-fluorinated P(BMA), attributed to the presence of fluorinated units conferring improved hydrophobic properties on a P(BMA-*co*-PFEHEMA) copolymer coating.

The aim of this work is the preparation of hydrophobic poly(meth)acrylates with different fluorinated side chains, such as poly(2,2,2-trifluoroethyl methacrylate) (PTFEMA) and poly(2-(perfluorohexyl)ethyl acrylate) (PPFEHEMA), by free radical polymerization. These polymers were characterized by <sup>1</sup>H and <sup>19</sup>F NMR and IR spectroscopy, WCA, DSC and TGA, and applied as coating materials to diammonium phosphate (DAP) fertilizers. The morphology and chemical composition of the coated fertilizer surfaces and cross-sections were investigated using SEM-EDX mapping, while a UV-visible spectrophotometer was utilized to monitor the release rates of phosphorus (P) and nitrogen (N) in water. Finally, the relationship between the structure of fluorinated polymers and the release profiles of N and P nutrients was studied to evaluate the performance in terms of slowing the release rate of nutrients through these fluorinated hydrophobic polymer coatings.



## 2. Experimental section

### 2.1. Materials

Diammonium phosphate (DAP) ((NH<sub>4</sub>)<sub>2</sub>HPO<sub>4</sub>) was chosen as a granular phosphate fertilizer to prepare SRFs. This commercial granular fertilizer, containing 46% phosphorus (P<sub>2</sub>O<sub>5</sub>) and 18% nitrogen (N), was generously provided by the OCP Group in Morocco. 2-(Perfluorohexyl)ethyl acrylate (PFEHEMA) (CAS: 17527-29-6) was kindly provided by Atofina (Pierre Bénite, France), while 2,2,2-trifluoroethyl methacrylate (TFEMA) was kindly supplied by Tosoh Finechemical Corp, Shunan, Yamaguchi (Japan). Azobisisobutyronitrile (AIBN) and all the solvents (hexafluorobenzene, acetonitrile, pentane, tetrahydrofuran, and methanol) were purchased from Sigma-Aldrich (France). Before use, TFEMA and PFEHEMA were purified by distillation under reduced pressure.

### 2.2. Synthesis of fluorinated homopolymers

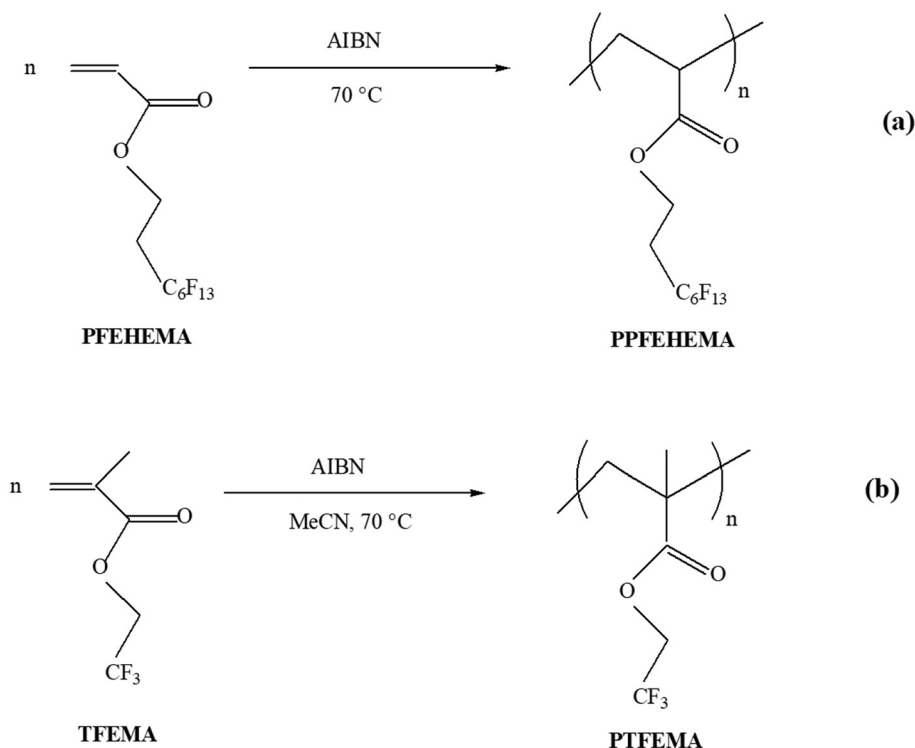
**2.2.1. Synthesis of poly(2-(perfluorohexyl)ethyl acrylate) (PPFEHEMA).** The bulk radical polymerization of 2-(perfluorohexyl)ethyl acrylate, PFEHEMA, was performed according to the procedure described by Stone *et al.*<sup>32</sup> Briefly, 12 mmol (5.03 g) of PFEHEMA monomer were placed in a glass flask equipped with a reflux condenser, thermometer, and a magnetic stirrer. AIBN as initiator (0.3 mmol, 2.5 mol% related to the monomer) was then added; the solution was purged with nitrogen gas for 15 min and heated in an oil bath at 70 °C for 24 h to complete the polymerization. After cooling the reactor, the final mixture was dissolved in hexafluorobenzene and pre-

cipitated from methanol. The obtained PPFEHEMA polymer was collected by filtration, washed with methanol, and dried under vacuum at 60 °C. The yield of PPFEHEMA (white powder) was close to 60%. The synthesis route of PPFEHEMA is displayed Scheme 1a.

**2.2.2. Synthesis of poly(2,2,2-trifluoroethyl methacrylate) (PTFEMA).** 2,2,2-Trifluoroethyl methacrylate (TFEMA) in acetonitrile (MeCN) was polymerized according to the same protocol described above (Scheme 1b). Briefly, 8 mL of MeCN, 36 mmol of TFEMA (6.02 g; 5.1 mL; 2.7 mol L<sup>-1</sup>) and 0.18 mmol of AIBN (0.06 g, 1 wt% of monomer) were used to charge a glass Schlenk flask reactor with a magnetic stirrer. After the polymerization reaction was complete, the resulting solid was solubilized in a minimal amount of tetrahydrofuran and then the resulting polymer was purified by precipitation in pentane and subsequently dried in an oven under vacuum at 50 °C. The yield of the obtained PTFEMA (white powder) was 75%.

### 2.3. Coating technique

To provide a suitable viscosity for a coating process, we prepared PTFEMA and PPFEHEMA polymer solutions in THF and hexafluorobenzene, respectively (in 40% w/v ratio). The commercially available granular DAP fertilizers were coated by a dip-coating process, as described in previous studies.<sup>9,31</sup> Dip-coating was achieved by immersing DAP granules (with diameters of 2–4 mm and a weight of *ca.* 35 mg) in the corresponding solutions for 10 min. The DAP pellets were then removed from solution and placed on a Teflon® film surface.



**Scheme 1** Radical polymerization of: (a) PFEHEMA and (b) TFEMA monomers.



Subsequently, the coated DAP granules were dried at room temperature, leading to a coated fertilizer with a single layer (1L). To create a coated DAP with a second layer (2L), this operation was repeated a second time on the coated DAP (1L) using the same coating solution.

The percentage coating (CC) was calculated according to the equation:

$$\text{CC\%} = \frac{m_f - m_i}{m_i} \times 100 \quad (1)$$

where  $m_f$  and  $m_i$  are the weights of the granular fertilizer after and before coating, respectively.

## 2.4. Characterizations

**2.4.1. Fourier-transform infrared spectroscopy (FTIR).** Powder samples were taken into KBr pellets. FTIR analyses were carried out using a PerkinElmer 1725X spectrometer in transmittance mode. The spectra were recorded at room temperature with scanning in the range 400–4000  $\text{cm}^{-1}$  with 16 acquisitions.

**2.4.2. Nuclear magnetic resonance (NMR) spectroscopy.** The  $^1\text{H}$  and  $^{19}\text{F}$  NMR spectra were recorded at room temperature using a Bruker AC 400 spectrometer at ambient temperature. Deuterated chloroform ( $\text{CDCl}_3$ ) and a 1:1 mixture of  $\text{CDCl}_3/\text{CF}_3\text{CO}_2\text{H}$  were used as NMR solvents for PTFEMA and PPFEHEMA, respectively. Chemical shifts are given in ppm.  $^1\text{H}$  and  $^{19}\text{F}$  NMR spectra were performed under the following experimental conditions: a flip angle of  $90^\circ$  for  $^1\text{H}$  ( $30^\circ$  for  $^{19}\text{F}$ ), acquisition time of 4.5 s (0.7 s), pulse delay of 2 s (5 s), 16 scans (64 for  $^{19}\text{F}$ ), and a pulse width of 5  $\mu\text{s}$  for  $^{19}\text{F}$  NMR.

**2.4.3. Size exclusion chromatography.** Size exclusion chromatography (SEC) analysis was carried out on a Polymer Laboratories PL-GPC 50 Plus instrument using 2 PL gel mixed-C 5  $\mu\text{m}$  columns (molar masses ranging from 200 to  $2 \times 10^6$   $\text{g mol}^{-1}$ ) thermostatted at  $35^\circ\text{C}$  equipped with a refractive index detector. Tetrahydrofuran (THF) with 1% LiBr was used as eluent ( $1.0 \text{ mL min}^{-1}$ ). The calibration was performed using Varian polymethylmethacrylate (PMMA) standards.

**2.4.4. Water contact angle (WCA) measurements.** Water contact angle (WCA) measurements were performed to investigate the degree of hydrophobic character of the synthesized fluorinated polymers. A KRUSS GmbH Easy Drop goniometer (Germany) equipped with a charge-coupled device camera was used to measure the contact angle of a water droplet in contact with a solid surface. An image capture program using SCAT software was utilized to record the measurements. To measure the contact angles, a circle was defined around the drop, and the tangent angle formed at the substrate surface was recorded. To ensure the reproducibility of the measurements, three experiments were conducted for each formulation.

**2.4.5. Thermogravimetric analysis (TGA).** To determine the thermal stability of the obtained polymers, TGA was performed on TA-55 discovery equipment. A few milligrams of each sample were heated at rate of  $10^\circ\text{C min}^{-1}$  from room temperature to  $800^\circ\text{C}$  under nitrogen gas ( $60 \text{ mL min}^{-1}$ ).

**2.4.6. Differential scanning calorimetry (DSC).** DSC analyses were performed on 10–15 mg samples under nitrogen flow on a Netzsch DSC 200 F3 instrument to observe thermal transitions using the following cycles: first heating from  $-60^\circ\text{C}$  to  $120^\circ\text{C}$  at  $10^\circ\text{C min}^{-1}$ , cooling from 120 to  $-60^\circ\text{C}$  at  $20^\circ\text{C min}^{-1}$ , and finally second heating from  $-60^\circ\text{C}$  to  $120^\circ\text{C}$  at  $10^\circ\text{C min}^{-1}$ . From the DSC thermograms (second heating), the inflection point of the step-change in heat capacity corresponds to  $T_g$ . An indium sample ( $T_m = 156.6^\circ\text{C}$ ) was used to calibrate the instrument.

**2.4.7. Scanning electron microscopy (SEM).** SEM analysis was recorded to characterize the morphology of uncoated and coated fertilizers, using a VEGA-3 instrument (TESCAN-France) with an accelerating voltage of 10 kV. Energy-dispersive X-ray (EDX) analysis was also used to identify the chemical composition of the coatings. Indeed, SEM was utilized to examine the maps of the spatial distribution of elements within the samples.

For this analysis, an axial rupture containing the fertilizer and the coating material was created using a razor blade. The coated granule and its cross-section were spread out on a carbon band and fixed to the surface of a metal disc using double-sided adhesive tape. Additionally, by examining the cross-sectional surface of coated DAP granular fertilizer, the coating thicknesses were determined.

**2.4.8. Release assays of nitrogen and phosphorus in water.** The P and N release profiles for the coated and uncoated TSP fertilizers were determined according to the protocol described in our previous work.<sup>9,31</sup> Briefly, uncoated and coated DAP granules (50 mg) were placed in a 125 mL beaker filled with distilled water and gently stirred at room temperature. Samples (100  $\mu\text{L}$ ) were collected at different time intervals, diluted 100 times, and analyzed in the spectrophotometer. Nitrogen ( $\text{NH}_4^+$ ) and phosphorus ( $\text{P}_2\text{O}_5$ ) release profiles were then conducted by a colorimetric process, using AFNOR-T90-015 and AFNOR-T90-023 norms, respectively. An ultraviolet-visible (UV-vis) spectrophotometer (UV-2600, Shimadzu) was used to characterize the resulting complex-colored solutions at 630 nm and 880 nm for  $\text{NH}_4^+$  and  $\text{P}_2\text{O}_5$ , respectively. The absorbance of all solutions was measured, and the standard curve was drawn. Linear fitting was undertaken and yielded correction equations of  $Y = 0.741X$  ( $R^2 = 0.997$ ) and  $Y = 0.615X$  ( $R^2 = 0.997$ ) for N and P nutrients, respectively.

## 3. Results and discussion

### 3.1. Preparation and characterization of PTFEMA and PPFEHEMA (coating materials)

For excellent weatherability, a semi-permeable membrane based on fluorinated acrylic polymers should be covered by as many fluorine-containing groups as possible.<sup>25,27,29,32</sup> In contrast to some low-molar-mass per- and polyfluoroalkyl substances (PFASs), well established as being water soluble, toxic, persistent, bioaccumulative and mobile, fluoropolymers are insoluble in water and thus not mobile, are bio-inert, safe and have unique properties that are essential for our daily lives





(coatings, electronics, internet of things, energy, transportation, etc.). Indeed, these materials are possibly irreplaceable, since suggested alternative products such as hydrocarbon polymers failed when used in similar conditions. Interestingly, these high-performance polymers satisfy the 13 polymer of low concern (PLC) criteria in their recommended conditions of use.<sup>33</sup> Therefore, these specialty polymers must be separated from the PFAS family. Shirai *et al.*<sup>34</sup> recently reported that poly (fluoroalkyl (meth)acrylate)s containing extended perfluoroalkyl groups ( $C_nF_{2n+1}$ ) can degrade, leading to the formation of perfluorooctanoic acid ( $C_7F_{15}CO_2H$ , PFOA). These authors also showed that polymers featuring short fluorinated side chains ( $n \leq 6$  fluorocarbons) present less bioaccumulative PFAS compared to those with  $n \geq 7$ . Therefore, taking in account the hydrophobic coating performances with fluorine-containing groups and to address environmental concerns with less bioaccumulation of PFOA, we have chosen to use TFEMA ( $-CF_3$ ) and PFEHEMA ( $C_6F_{13}$ ) as fluorinated monomers to prepare PTFEMA and PPFEHEMA polymers with high molar masses compared to those of PFASs, which can be applied as coating fertilizers to achieve the slow release of nutrients. These polymers were successfully synthesized by free radical polymerization (Scheme 1). The resulting polymers were then analyzed, and finally used as coating materials to cover diammonium phosphate (DAP) fertilizers.

**3.1.1. Infrared spectroscopic analysis (FTIR).** Fig. S1 (ESI<sup>†</sup>) shows the FTIR spectra of the TFEMA and PFEHEMA monomers and the corresponding PTFEMA and PPFEHEMA homopolymers. Fig. S1<sup>†</sup> displays the characteristic FTIR absorption peaks assigned to different chemical bonds, as summarized in Table 1. These assignments agree with those of fluorinated (meth)acrylate polymers described in the literature.<sup>35–39</sup> Meanwhile, the characteristic stretching of the TFEMA and PFEHEMA double bond observed at 1649 and 1638  $cm^{-1}$ , respectively, disappeared, indicating that the polymerization reaction and purification of the resulting polymers had been successfully achieved.

**3.1.2  $^1H$  and  $^{19}F$  NMR spectroscopy.** The white powders (purified copolymers) were characterized by NMR spectroscopy. Fig. 1 provides the  $^1H$  and  $^{19}F$  NMR spectra of the PTFEMA polymer recorded in deuterated chloroform, while the NMR spectra of PPFEHEMA were recorded in a 1:1 mixture of  $CDCl_3/CF_3CO_2H$ , since PPFEHEMA is not soluble in organic solvents.

**Table 1** Principal FTIR characteristic bands of PTFEMA and PPFEHEMA polymers

Band	PTFEMA ( $cm^{-1}$ )	PPFEHEMA ( $cm^{-1}$ )
C–F symmetric stretching	1225	1202
C–F asymmetric stretching	1176	1145
C=O ester stretching	1753	1737
C–H: symmetric and asymmetric stretching	2850 and 2960	2875 and 2972
C–H (out of plane)	973	844
C–O stretching	1176	1116

The assignments of the chemical shifts were derived by comparison with the values reported in the literature for TFEMA-based polymers<sup>38</sup> and poly(perfluoro(meth)acrylate)s<sup>29</sup> and are summarized in Table 2. For example, the  $^1H$  NMR spectrum of PTFEMA shows a signal of the methylene of ester group ( $-O-CH_2-CF_3$ ) centered at 4.3 ppm. The methyl group of PTFEMA ( $-CH_3$ ) was observed in the range 0.8–1.1 ppm, while the methylene protons of the backbone ( $CH_2$ ) appear between 1.8 and 2.1 ppm. The  $^{19}F$  NMR spectrum of PTFEMA exhibits the  $CF_3$  peak at  $-73$  ppm. The vinylic proton signal centred at 6.1 ppm for TFEMA and peaks at 6.5, 5.9 and 5.0 for PFEHEMA were not present in these spectra.

**3.1.3. Size exclusion chromatography.** The molar masses of poly(2,2,2-trifluoroethyl methacrylate), PTFEMA, were determined using size exclusion chromatography (SEC) in tetrahydrofuran (THF), calibrated with polymethylmethacrylate (PMMA) standards. The obtained  $\bar{M}_n$  and  $\bar{M}_w$  and dispersity ( $D = \bar{M}_w/\bar{M}_n$ ) values are equal to 26 000  $g\ mol^{-1}$ , 52 000  $g\ mol^{-1}$  and 2.0, respectively. Of course, these are relative values. However, it is not possible to determine the molar masses of poly(2-(perfluorohexyl)ethyl acrylate) (PPFEHEMA) as it is not soluble in organic solvents, but only in fluorinated solvents such as hexafluorobenzene or 1,1,1,3,3,3-hexafluoro-2-propanol. Actually, our SEC apparatus is not equipped with columns related to fluorinated solvents.

**3.1.4. Water contact angle (WCA).** WCA is one of the most important parameters affecting release kinetics since the hydrophilic character of polymer films reduces the diffusion of water through these films and gives them water-repellent properties.<sup>40</sup> The WCA value for the PTFEMA film was about  $97^\circ$ , while that of PPFEHEMA reached a value of  $119^\circ$ , as shown in Fig. S2 (ESI<sup>†</sup>). The difference in WCA between the two homopolymers ( $22^\circ$ ) indicates a more pronounced hydrophobic character for PPFEHEMA film compared to PTFEMA film. This can be attributed to the difference in the surface energy value in the chemical structure at the surface of both fluorinated polymers.<sup>39</sup> Barbu *et al.*<sup>41</sup> reported that the constituent groups affect the surface energy in the following order:  $CH_2$  (36  $mN\ m^{-1}$ ) >  $CF_2$  (23  $mN\ m^{-1}$ ) >  $CF_3$  (15  $mN\ m^{-1}$ ). Tsibouklis *et al.*<sup>42</sup> also studied the surface organization phenomena and the surface energy of poly(perfluoroalkyl methacrylate)s films. They observed the influence of the length of the pendant fluorocarbon moiety on the surface energy, and concluded that increasing the chain length induces a lower surface energy. Indeed, as the pendant chain length increases, the average surface roughness ( $R_a$ ) of the corresponding film structures, determined by AFM, follows the same trend, and therefore serves to inhibit the absorption of liquids by the bulk sample.<sup>42</sup> In fact, the  $R_a$  value of PPFEHEMA is close to 3.1 nm (ref. 42) while that of PTFEMA is 0.41 nm.<sup>43</sup> The surface properties of comb-shaped polymers with perfluoroethyl side chains ( $R_f$ ) are also strongly related to the ordered structure of the side chains at the surface. Our team reported the thermal behavior, liquid-crystalline structure, and functional group orientation of comb-shaped polymers poly(2-(perfluorooctyl)ethyl acrylate) containing perfluorooctyl side chains.<sup>24</sup> A tilted



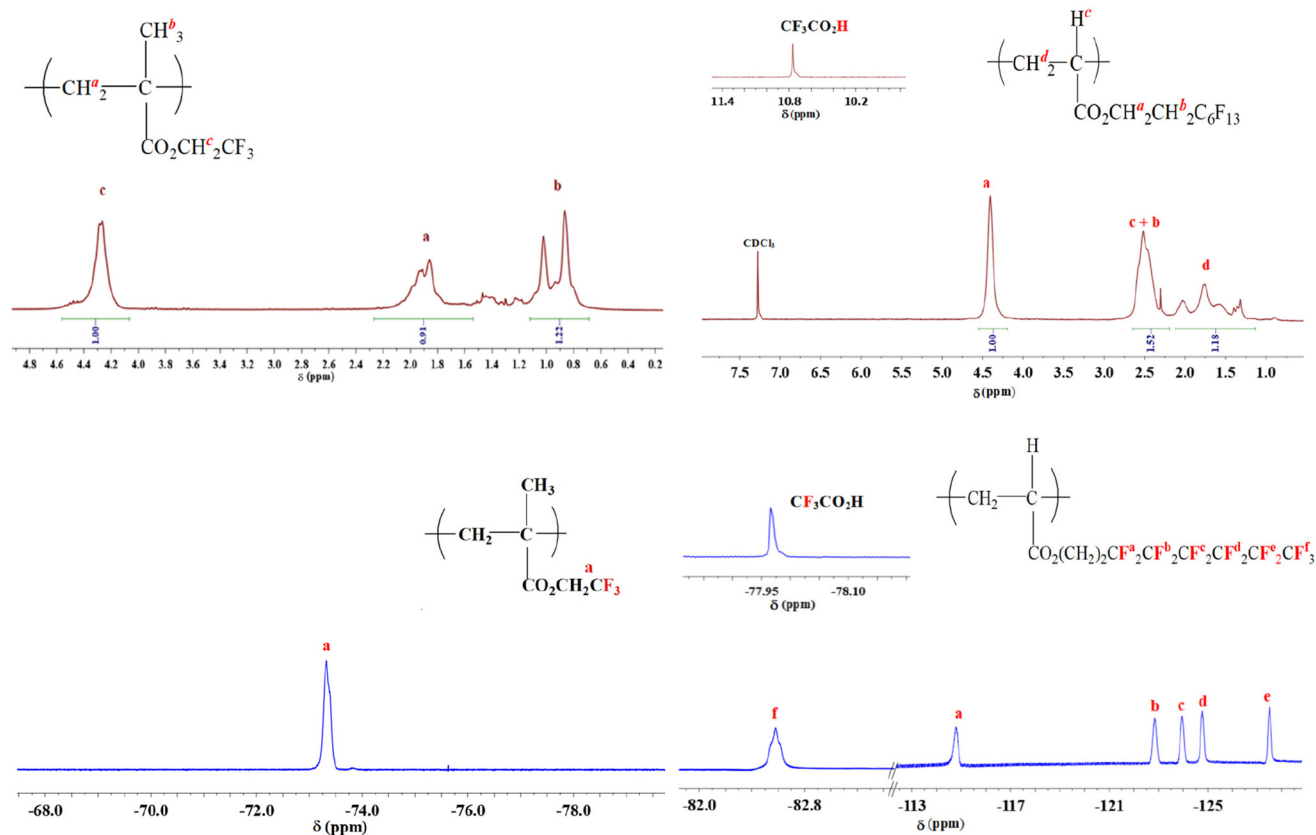


**Fig. 1**  $^1\text{H}$  and  $^{19}\text{F}$  NMR spectra of PTFEMA (left) ( $\text{CDCl}_3$  as the solvent) and PPFEHEMA (right) (a mixture of  $\text{CDCl}_3$  and  $\text{CF}_3\text{COOH}$  as NMR solvent in  $^1\text{H}$ -( $^{19}\text{F}$ ) decoupling mode NMR (chemical shifts in the inserts correspond to  $\text{CF}_3$  and  $\text{CO}_2\text{H}$  groups).

**Table 2** Assignments of chemical shifts/ppm for PTFEMA and PPFEHEMA polymers

Type of proton	PTFEMA	PPFEHEMA
<b><math>^1\text{H}</math> NMR</b>		
$\text{CH}_3$	0.8–1.1	—
$\text{CH}_2$ (main chain)	1.8–2.1	1.2–2.2
$\text{CH}$ (main chain)	—	2.2–2.7
$\text{OCH}_2\text{CF}_3$	4.3	—
$\text{OCH}_2\text{CH}_2\text{C}_6\text{F}_{13}$	—	4.2–4.5
$\text{OCH}_2\text{CH}_2\text{C}_6\text{F}_{13}$	—	2.2–2.7
<b>Type of fluorine</b>		
<b><math>^{19}\text{F}</math> NMR</b>		
$\text{OCH}_2\text{CF}_3$	−73.0	—
$\text{O}(\text{CH}_2)_2\text{CF}_2\text{CF}_2\text{CF}_2\text{CF}_2\text{CF}_2\text{CF}_3$	—	−114.8
$\text{O}(\text{CH}_2)_2\text{CF}_2\text{CF}_2\text{CF}_2\text{CF}_2\text{CF}_2\text{CF}_2\text{CF}_3$	—	−124.8
$\text{O}(\text{CH}_2)_2\text{CF}_2\text{CF}_2\text{CF}_2\text{CF}_2\text{CF}_2\text{CF}_2\text{CF}_3$	—	−122.8
$\text{O}(\text{CH}_2)_2\text{CF}_2\text{CF}_2\text{CF}_2\text{CF}_2\text{CF}_2\text{CF}_2\text{CF}_3$	—	−123.9
$\text{O}(\text{CH}_2)_2\text{CF}_2\text{CF}_2\text{CF}_2\text{CF}_2\text{CF}_2\text{CF}_2\text{CF}_3$	—	−127.5
$\text{O}(\text{CH}_2)_2\text{CF}_2\text{CF}_2\text{CF}_2\text{CF}_2\text{CF}_2\text{CF}_2\text{CF}_3$	—	−82.6

hexatic smectic-B phase was obtained, with the  $R_f$  side chains playing the role of mesogens to form a bilayer lamellar structure with lateral hexagonal translational order producing a well-ordered structure, which exhibits better liquid repellency than those analogues with short fluorinated chains. According

to the different parameters involved above, the hydrophobic characteristic of the fluorinated polymer, PPFEHEMA, was improved compared to that of PTFEMA, based on the fluorinated chain length with a lower surface energy, a high average surface roughness ( $R_a$ ) and the well-ordered structure of PPFEHEMA. This result is in good agreement with previous work.<sup>31,44</sup> Comparing two fluoroalkyl methacrylate polymers, Phillips and Dettre<sup>44</sup> found that a polymer bearing a longer fluoroalkyl side chain displays the highest WCA value.

**3.1.5. Thermal properties (TGA and DSC).** DSC and TGA analyses were used to study the thermal properties of PTFEMA and PPFEHEMA (Fig. 2).

The degradation of PTFEMA takes place in two steps (Fig. 2a). The first one, in the range 200–300 °C, corresponds to the volatilization of side-chain fragments, including  $\text{CO}_2$ , vinylidene fluoride and 2,2,2-trifluoroethanol, which are determined to be pyrolytic decomposition products (weight loss 26%). The second decomposition step, in the range 305–420 °C (weight loss 74%), is attributed to a depolymerization reaction.<sup>45,46</sup> PPFEHEMA decomposes in a single step, in the range 280–420 °C, which is attributed to a random cleavage leading to a depolymerization mechanism (Fig. 2a). PPFEHEMA exhibits higher thermal stability than PTFEMA (Fig. 2a), which can be attributed to the better thermal stability of the  $\text{C}_6\text{F}_{13}$  pendant group in PPFEHEMA due to the strong



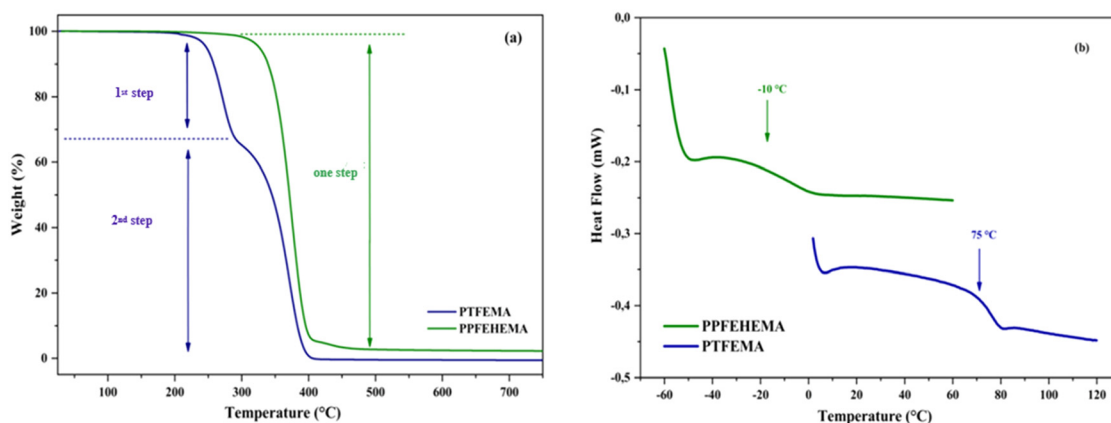


Fig. 2 TGA (a) and DSC (b) thermograms of PTFEMA and PPFEHEMA ( $N_2$  gas).

C–F bond ( $E_{C-F} = 450 \text{ kJ mol}^{-1}$ ) that makes it possible to increase the heat resistance performance of the polymeric materials by adding more fluorinated components.<sup>31</sup> Table 3 lists the thermal characteristics of PTFEMA and PPFEHEMA.

The DSC second heating thermograms of both fluorinated polymers showed no melting temperature when the samples were heated from  $-60 \text{ }^\circ\text{C}$  to  $120 \text{ }^\circ\text{C}$  (Fig. 2b). Only a sharp transition from the glassy state to the viscoelastic one was observed, as evidenced by the presence of a neat  $T_g$ , indicating that these fluorinated polymers exhibited amorphous behavior (Table 3); the  $T_g$  were close to  $-10$  and  $75 \text{ }^\circ\text{C}$  for PPFEHEMA and PTFEMA, respectively.

The decrease in  $T_g$  for PPFEHEMA compared to PTFEMA is related to the structure of the PFEHEMA units. In fact, the long alkyl dangling chains of the acrylate moiety ( $-\text{CO}_2\text{CH}_2\text{CH}_2\text{C}_6\text{F}_{13}$ ) serve as internal plasticizers, resulting in low  $T_g$  and giving PPFEHEMA a more elastomeric behavior at room temperature, as shown in Fig. S3.†<sup>47</sup> The decrease in  $T_g$  leads to excellent film-forming properties at room temperature for fertilizer coating. The PPFEHEMA coating films also help to improve the physical quality of granular fertilizer and are expected to have a positive effect on their compressive strength so that they do not break easily, preventing the generation of excessive dust during the handling and storage process.

### 3.2. Morphological characterization of coated DAP fertilizers

Film forming from polymer solution coatings for DAP fertilizers was performed using the dip-coating method.<sup>9,30</sup> The per-

centages of the different coating materials (calculated according to eqn (1)) are given in Table 4.

To investigate the quality of the coating between the fertilizer and the coating, the morphology of the surface and the cross-section of uncoated and PTFEMA and PPFEHEMA coated DAP with a single layer (1L) and a second layer (2L) was investigated by SEM (Fig. 3).

A first overview of the SEM results showed that the surface of the uncoated DAP granule has an irregular and rough structure (Fig. 3a; scale bar: 1 mm).

The highly magnified surface (Fig. 3a; scale bar:  $100 \mu\text{m}$ ) showed some pinholes and an irregular morphology, due to the granulation process during the production of DAP fertilizers.<sup>40,48</sup> When the DAP fertilizer was coated with the two PTFEMA and PPFEHEMA polymers, the coating surfaces exhibited a smoother and denser structure compared to uncoated DAP, especially when the fertilizers were covered with the second layer, as the content of the coating membrane on the surface of the fertilizers increased (Fig. 3b–d). This is in good agreement with our previous work.<sup>9,31,40,48,49</sup>

When analyzing the outer surface of the DAP granules coated with PTFEMA (Fig. 3b and c), we found that there are some microcracks in the surface compared to the granules coated with PPFEHEMA, which may be related to the structure of these polymers. PPFEHEMA has a  $T_g$  that is lower than the ambient temperature ( $-10 \text{ }^\circ\text{C}$ ), so the PPFEHEMA coating has high flexibility and good film-formation, resulting in improved impact and crack resistance (Fig. S3†). In contrast, PTFEMA with a  $T_g$  of around  $70 \text{ }^\circ\text{C}$  (Table 3) exhibits a glassy state at

Table 3 Thermal data of PTFEMA and PPFEHEMA by TGA and DSC

Polymer	TGA <sup>a</sup>			DSC $T_g$ ( $^\circ\text{C}$ )
	$T_{d10\%}$ ( $^\circ\text{C}$ )	$T_{d50\%}$ ( $^\circ\text{C}$ )	Residue at $600 \text{ }^\circ\text{C}$ (%)	
PTFEMA	256	345	0.0	75
PPFEHEMA	339	371	2.0	-10

<sup>a</sup>  $T_{dx\%}$ : temperature of  $x\%$  of decomposition ( $N_2$  gas,  $10 \text{ }^\circ\text{C min}^{-1}$ ).

Table 4 Percentages of coating materials, PTFEMA and PPFEHEMA, with different layers (L)

DAP coating	Weight coating percentage (%)	Average thickness ( $\mu\text{m}$ )
PTFEMA 1L	4.5	51.0
PTFEMA 2L	10.7	90.0
PPFEHEMA 1L	7.7	27.0
PPFEHEMA 2L	16.0	73.0



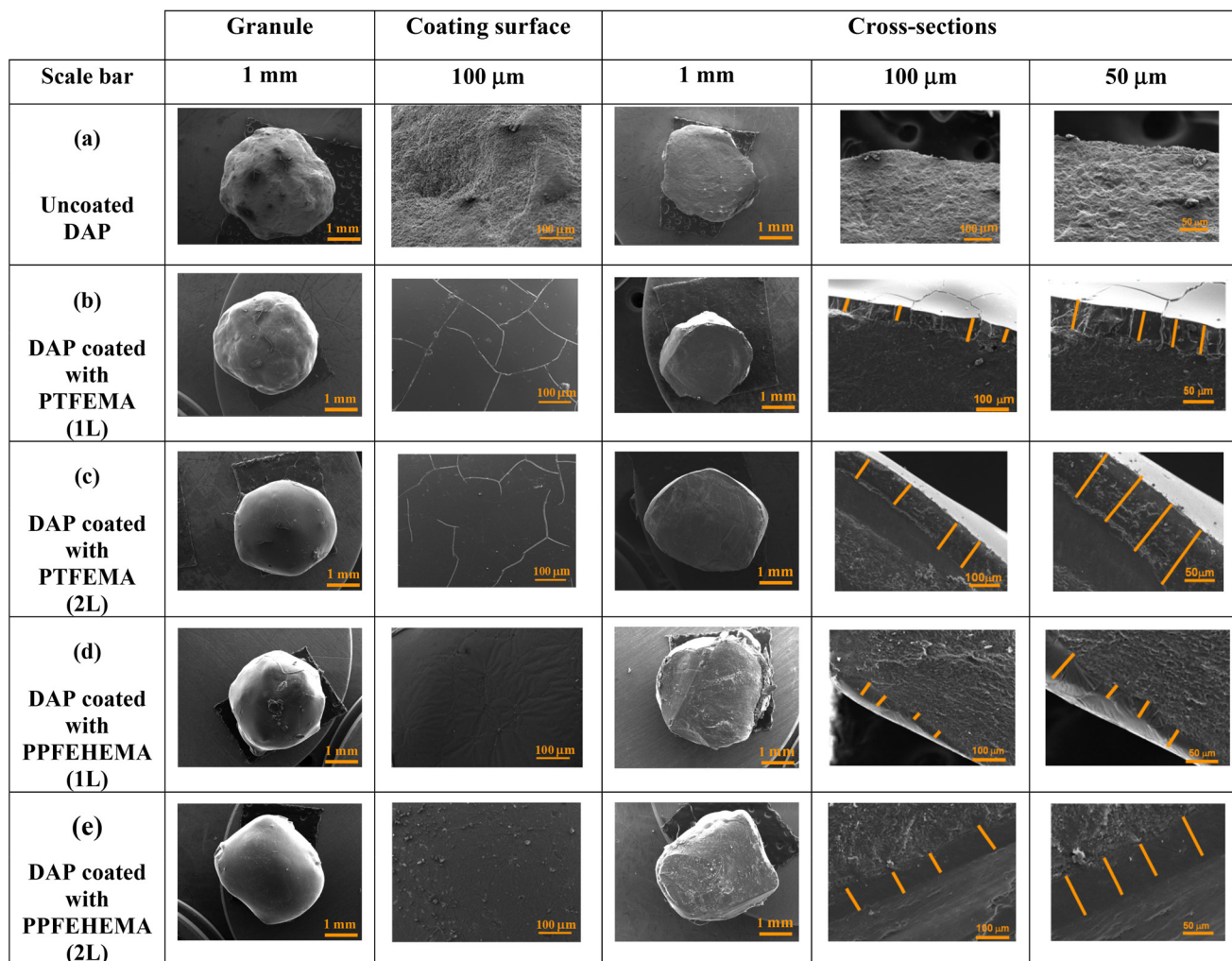


Fig. 3 SEM analysis of a fertilizer granule and its cross-section containing the interface between DAP and tested PTFEMA and PPFEHEMA (single layer (1L) and second layer (2L)).

room temperature, which leads to some cracking when the solvent evaporates. These cracks could be reduced when the second layer was applied to the surface of the coated fertilizer. To eliminate these cracks or prevent their formation, Devassine *et al.*<sup>50</sup> reported that controlling the rate of solvent evaporation or performing annealing could prevent the formation of cracks and pores. Yadavalli *et al.*<sup>51</sup> observed some cracks in the SEM of the composite thin films and reported another explanation, which is the electron-beam-induced rapid volatilization of the organic species, such as residual solvent from the surface of these films during SEM analysis, leading to a buildup of tensile stress that causes cracks in the grain boundaries.

The cross-sectional images of coating materials observed by SEM with different magnitudes are shown in Fig. 3b–e. The contact surface between PTFEMA or PPFEHEMA (1L and 2L) coatings and the DAP core fertilizers is continuous with no gaps or voids present within it. In fact, the interaction between the hydrophilic inorganic DAP granules ( $(\text{NH}_4)_2\text{HPO}_4$ ) and the

hydrophilic side (ester groups  $-\text{CO}_2-$ ) in the PTFEMA and PPFEHEMA coatings could be responsible for the good adhesion by both compounds.<sup>47</sup> Indeed, the border lines between fertilizer and the film coatings are irregular due to the non-spherical irregular shape of the initial DAP granules (Fig. 3b and d; scale bar: 100  $\mu$ m). Poly(fluorinated (meth)acrylate)s are a viable option for use in agriculture as coatings for SRFs, as confirmed by the formation of cohesive films.<sup>31</sup>

From the cross-section of core (fertilizer)–shell (coating) (Fig. 3b–e), the thicknesses of polymer coating were assessed by SEM at different points due to the irregular shape of DAP fertilizers, and the average thicknesses were calculated (Table 4). These values are a function of the type of coating (PTFEMA or PPFEHEMA) and their content (1L or 2L), as displayed in Fig. S4.†

The thicknesses of the different PTFEMA and PPFEHEMA coatings are also shown in Fig. S4.† The average thicknesses of DAP coated with PTFEMA (1L) and (2L) are close to 51 and 90  $\mu$ m, respectively, while those achieved when PPFEHEMA is





used as the coating are around 27 and 73  $\mu\text{m}$  for 1L and 2L, respectively. The measured thicknesses of the two-layer (2L) coating are 1.5 and 2.7 times higher than those of the single-layer (1L) PTFEMA and PPFHEMA coatings, respectively.

Energy dispersive X-ray analysis (EDX) was used to reveal the chemical compositions on the surface of the coated and uncoated DAP fertilizers to evaluate the quality of the coatings. The results are shown in Fig. 4 and Table 5.

As essential macronutrients, the N and P signals of the DAP fertilizer were detectable only on the uncoated DAP surface. Their percentages were 21.55% and 10.10%, respectively (Table 5). Other microelements with a low content (0.67%), including Mg, Al and Ca, were also observed. The signal related to carbon (19.54%) was related to the metallization of DAP granules because the samples needed to be conductive to perform the SEM analysis.

The absence of N and P macronutrients on the outer surface of the coated DAP granules confirms that the PTFEMA

and PPFHEMA coatings covered the granular fertilizers successively with good adhesion and without any diffusion of the macronutrients N and P of the DAP fertilizer. These results are also corroborated by the SEM analyses. In the DAP coated with PTFEMA and PPFHEMA membranes, the carbon content increases compared to that of the non-coated DAP fertilizer, which is attributed to the carbon atoms in the fluorinated (meth)acrylate units of the polymer coatings. As expected, the DAP coated with PPFHEMA has a higher percentage of F-atoms than that coated with PTFEMA (Table 5 and Fig. 4).

The spatial distribution of the elements was investigated using the EDX technique. For example, Fig. 5 shows the element mapping (C, N, P, O and F) in the cross-section of DAP encapsulated with PPFHEMA 2L. The C, N, P, O and F are the constituent elements of the core-shell that display a more homogeneous distribution on the cross-section of DAP coated with PPFHEMA.

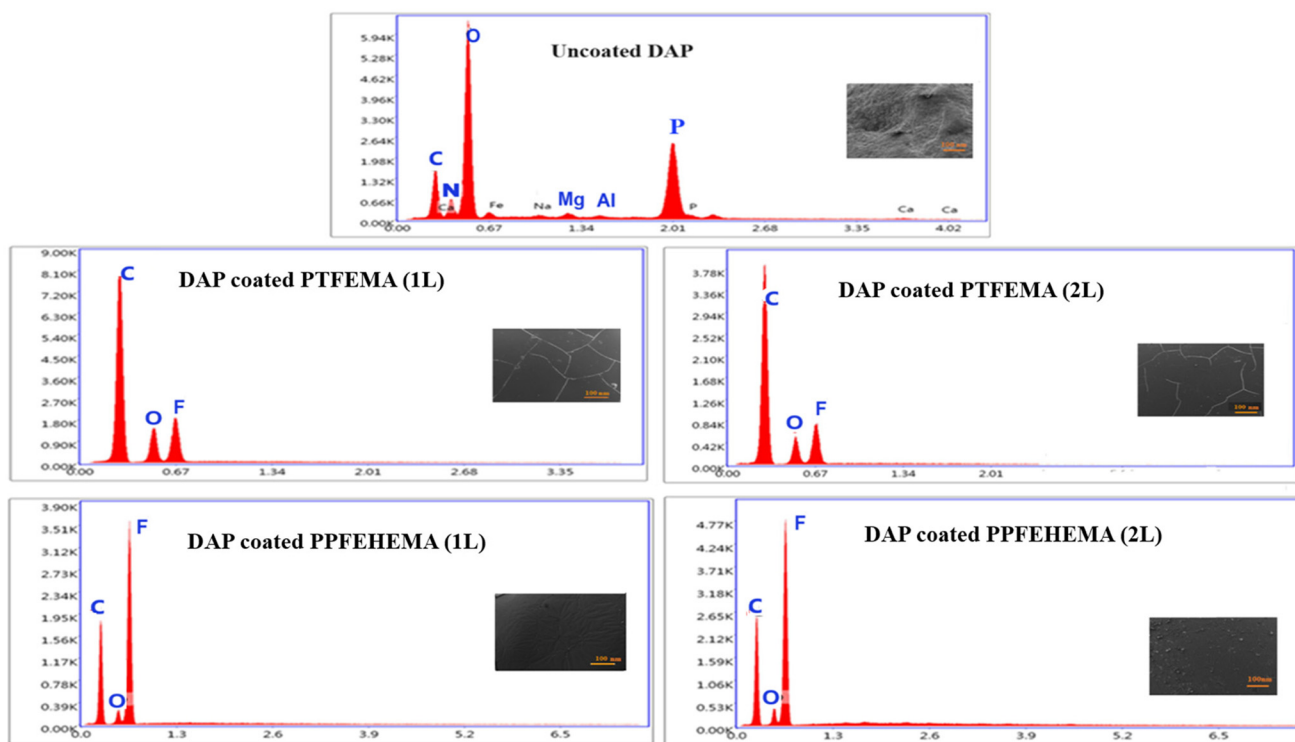


Fig. 4 EDX analysis on the surface of uncoated DAP and DAP coated using PTFEMA and PPFHEMA 1L and 2L.

Table 5 EDX elemental weight percentages of uncoated and coated DAP with different tested polymers (1L and 2L)

		Detected nutrients (wt%)					
		C	F	O	N	P	Other elements
Uncoated DAP		19.54	0	46.98	10.10	21.55	0.67
DAP coated with PTFEMA	1L	67.03	15.42	17.55	0	0	0
	2L	73.41	14.37	12.21	0	0	0
DAP coated with PPFHEMA	1L	44.28	50.12	05.59	0	0	0
	2L	44.79	49.57	05.64	0	0	0



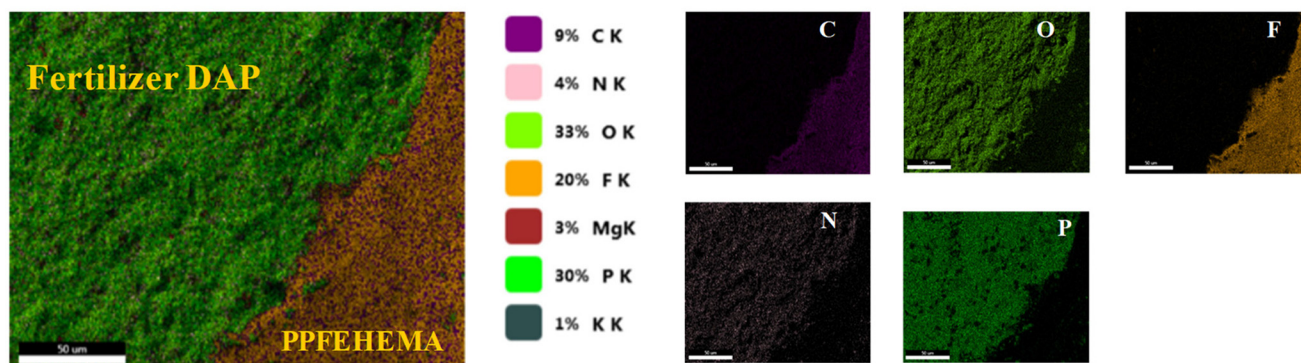


Fig. 5 Chemical mapping obtained from the cross-sections of DAP coated with PPFEHEMA (2L) (scale bar: 10  $\mu\text{m}$ ).

### 3.3. Phosphorous and nitrogen release behavior of coated and non-coated DAP fertilizers

To predict slow macronutrient releases for practical application, the nitrogen (N) and phosphorus (P) release patterns of uncoated and coated DAP fertilizer granules in water were studied according to the procedures described by Li *et al.*<sup>52</sup> and Pereira *et al.*<sup>53</sup> This allows an evaluation of the effects of the coating on the slow release and retarding performance of the coatings. The total percentage releases of P and N in water *versus* time for the uncoated and DAP coated with PTFEMA or PPFEHEMA polymers (1L or 2L) at pH 7 and ambient temperature are shown in Fig. 6.

Fig. 6 shows that the uncoated DAP is completely dissolved in water in less than 2 h, whereas the rate of dissolution of nutrients in water is much slower with the encapsulated fertilizers than with uncoated DAP. For example, the times to reach the maximum percentage release of P are 3.3 and 14.5 times higher than for uncoated DAP when the fertilizer is covered with PTFEMA single-layer (1L) and double-layer (2L), respectively.

When the DAP was coated with PPFEHEMA 1L and 2L, respectively, the P release profiles of the coated granules reached the equilibrium stage at approximately 7.5 h and

50.5 h, indicating significantly slower P release or delaying performance properties of DAP fertilizers, and thus their potential applications as coating films in crop agriculture.<sup>31,40,47,48</sup> DAP coated with 2L of PPFEHEMA presents the slowest macronutrient release: the times to reach the maximum N and P release are 30 and 38 times higher than those of uncoated DAP, respectively. Indeed, compared to PTFEMA, the PPFEHEMA coating shows significantly slower release of nutrients (Fig. 6 and Fig. S5<sup>†</sup>). In fact, the chemical structure of the coating is one of the key parameters determining the release rate of P nutrient from the coating. The presence of a larger number of F atoms and C–F bonds in the PFEHEMA monomer with hydrophobic properties, attributed to the  $-\text{C}_6\text{F}_{13}$  side groups, gives the PPFEHEMA coating a very hydrophobic character, that acts as a physical barrier and reduces water diffusion, contributing to the slow release of P and N nutrients compared to PTFEMA-coated DAP.<sup>21,22,26</sup> This hydrophobic character was confirmed by water contact measurement (WCA) (Fig. S2<sup>†</sup>), where the value of PPFEHEMA (WCA = 109°) is higher than that of PTFEMA (WCA = 79°). The soft structure of PPFEHEMA, which was confirmed by DSC (Fig. 2b and Table 3) gives the polymer good film-forming ability and good adhesion properties.<sup>31</sup>

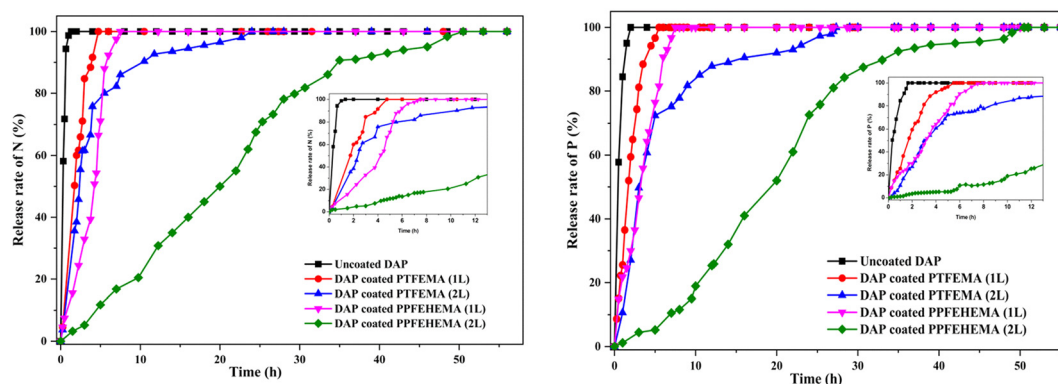


Fig. 6 Release rate of P and N for uncoated DAP and coated DAP using PTFEMA and PPFEHEMA 1L and 2L in water at pH = 7 and ambient temperature.



Another important parameter that can contribute significantly to nutrient release is the thickness of the coating. A greater thickness of these coatings resulted in lower nutrient release, as the coating film creates diffusion resistance to water and hinders nutrient diffusion. According to da Cruz *et al.*,<sup>54</sup> DAP coated with 3.0 and 4.5 wt% of polyurethane prepared from castor oil polyol showed a notable delay in phosphorus release. 80% of P was released in 50 h and 75 h when the coating percentage was close to 3.0 wt% and 4.5 wt%, respectively. In our case, the results indicated that thicker PPFEHEMA coatings may shift the maximum nutrient availability towards longer periods. The maximum release rate of P was reached after 7.5 h for DAP coated with a single layer (1L) (thickness = 27  $\mu\text{m}$ ), whereas that covered with a double-layer (2L) coating (thickness = 73  $\mu\text{m}$ ) resulted in a maximum release after 50.5 h (Fig. S5†).

To enhance the efficiency of fertilizer use and to minimize adverse environmental effects, the performance in terms of slow-release nutrients of fertilizer coatings is governed by extending nitrogen (N) and phosphorus (P) release properties by delaying the time to reach equilibrium, and therefore matching nutrient demand during crop growth. A comparison of P release times at equilibrium of PTFEMA and PPFEHEMA coatings with various previous studies using acrylate coating polymers is given in Table 6.

Using the immersion method, the P release profiles of the fertilizers coated with PPFEHEMA reached the equilibrium stage after 50 h, longer than those encapsulated with poly (butyl methacrylate (BMA)-*co*-PFEHEMA) (*ca.* 32 h). This copolymer was synthesized by emulsion copolymerization from an initial ratio of  $[\text{BMA}]_0/[\text{PFEHEMA}]_0 = 90/10$ .<sup>31</sup> Indeed, the molar incorporation of PFEHEMA in the copolymer, assessed by elemental analysis, was close to 6.5%<sup>31</sup> which is much lower than that of PFEHEMA units in the PPFEHEMA homopolymer (100%). The structure and hydrophobic properties of PFEHEMA homopolymer and P(BMA-*co*-PFEHEMA) copolymer coatings could explain the difference in their slow-release performance. In fact, PPFEHEMA (*i.e.*, with a high PFEHEMA molar percentage) compared to that incorporated in poly(BMA-*co*-PFEHEMA) (only 6.5%) exhibits a higher hydrophobic character, as confirmed by WCA measurements, of close to 110° and 80°, respectively.<sup>31</sup> Table 6 also reveals that DAP coated with PPFEHEMA exhibits a slower P release than that covered

with PBMA. The time to reach the maximum P release of the granule encapsulated with PPFEHEMA was 2.0 times lower than that of DAP coated with PBMA. The increasing hydrophobicity of the fluorinated homopolymer (WCA = 110°, Fig. S2†) compared to that of non-fluorinated PBMA (WCA = 74°)<sup>31</sup> suggests a reduction in water diffusion and contributes to the slow release of P nutrient due to the presence of the fluorinated comonomer bringing about better water repellency attributed to the  $-\text{C}_6\text{F}_{13}$  side groups.

This comparison shows that the release properties of PPFEHEMA 2L lead to better results thanks to its fluorinated structure, which improves the slow release of nutrients and avoids the loss of nutrients and their negative impact on the environment when uncoated fertilizer is used. Therefore, the better bioavailability of N and P nutrients is better for plants.

### 3.4. Mathematical modeling of release kinetics

To confirm the above interpretations of the behavior of nutrient release in water and to describe the release kinetics and the nutrient transport mechanism through the polymer coatings, data curves (Fig. 6) were fitted following the semi-empirical Ritger–Peppas model<sup>55</sup> (eqn (S1) in ESI†). More details about this model and the corresponding mechanisms based on the diffusional exponent ( $n$ ) characterizing the release mechanism are supplied in ESI.†

The diffusion exponent ( $n$ ), correlation coefficient ( $R^2$ ) and release factor ( $k$ ) of each coating system were calculated by plotting  $\ln(M_t/M_\infty)$  versus  $\ln(t)$ . Fig. S5† exhibits some of the curves (according to eqn (S2) in ESI†) while Table 7 supplies the resulting data for N and P nutrient releases from both polymers corresponding to the first and second layers for the first release step before reaching equilibrium.

PTFEMA and PPFEHEMA with a double layer (2L) present a Fickian release mechanism for P nutrient as their  $n$  values (0.52 and 0.48) are close to 0.5. However, those corresponding to N nutrient are greater than 1, indicating that the diffusion occurred from the pores in the coatings, which gradually become modified by the diffusion process itself. Furthermore, both PTFEMA and PPFEHEMA with 2L display a non-Fickian release mechanism for P nutrient as their  $n$  values range between 0.5 and 1.0 while for those corresponding to N release, the  $n$  values are greater than 1.

**Table 6** Comparison with previously published results for poly(acrylate) coating materials

Coating fertilizer <sup>a</sup>	Coating process	Total release of (P <sub>2</sub> O <sub>5</sub> ) in water (hours)	Ref.
Uncoated DAP	—	2.0	—
DAP coated with starch nanocrystal/PBMA	Immersion	25.2	31
DAP coated with starch nanocrystal/P(BMA- <i>co</i> -PFEHEMA)	Immersion	32.5	31
DAP coated with polymethyl methacrylate- <i>g</i> -carboxymethyl cellulose	Rotary pan	30.0	49
PMMA	Rotary pan	23.0	49
DAP coated with PTFEMA (double layer)	Immersion	24.0	This work
DAP coated with PPFEHEMA (double layer)	Immersion	50.5	This work

<sup>a</sup> BMA: butyl methacrylate, PFEHEMA: 2-(perfluorohexyl)ethyl acrylate and TFEMA: 2,2,2-trifluoroethyl methacrylate and PMMA: poly(methyl methacrylate).



**Table 7** Kinetic parameters of N and P releases in water calculated according to the Ritger–Peppas model from DAP coated with PTFEMA and PPFEHEMA 1L and 2L

			Release exponent, $n^a$	Release factor, $k \times 10^2$ (h <sup>-1</sup> )	Correlation coefficient ( $R^2$ )	Release mechanism
DAP coated	PTFEMA (1L)	P	0.96	57	0.98	Non-Fickian
		N	0.65	65	0.99	Non-Fickian
	PPFEHEMA (1L)	P	0.78	51	0.97	Non-Fickian
		N	1.30	34	0.97	—
DAP coated	PTFEMA (2L)	P	0.52	51	0.97	Fickian
		N	1.28	46	0.97	—
	PPFEHEMA (2L)	P	0.48	46	0.98	Fickian
		N	1.29	32	0.98	—

<sup>a</sup> Assessed from eqn (S2) (ESI†).

It is also noted that the  $k$  release factor values of P and N nutrients decreased for both PTFEMA and PPFEHEMA polymers when the percentage of coating or the layer coating number increased and *vice versa*. For example, when the DAP was coated with PTFEMA,  $k$  value of P release decreased from  $57 \times 10^{-2}$  to  $51 \times 10^{-2}$  h<sup>-1</sup> while the percentage of coating increased from 4.5% to 10.7% for PTFEMA 1L and PTFEMA 2L, respectively. Compared to the PTFEMA coating, PPFEHEMA exhibits slower N and P release profiles when using the same number of layers, and the  $k$  value of P release decreased from  $51 \times 10^{-2}$  to  $46 \times 10^{-2}$  h<sup>-1</sup>, while those of N release decreased from  $46 \times 10^{-2}$  to  $32 \times 10^{-2}$  h<sup>-1</sup> for PTFEMA 2L to PTFEMA 1L, respectively (Table 7). This attests to the nutrient releases being slower when DAP was coated with PPFEHEMA. This comparison is in good agreement with the release rates of N and P coated with both fluorinated polymers *versus* time (Fig. 6). Indeed, according to the WCA measurements, fluorinated PPFEHEMA is more hydrophobic than PTFEMA and therefore the swelling content is lower than that of PTFEMA leading to a low release factor  $k$  value.

## 4. Conclusions

Poorly bioaccumulative fluorinated (meth)acrylic polymers were used as hydrophobic coating materials for granular water-soluble fast-acting fertilizers. PTFEMA and PPFEHEMA were successfully synthesized, characterized, and applied to DAP fertilizers. PPFEHEMA, with a highly hydrophobic character due to the presence of a large number of fluorine atoms on the side chain (–C<sub>6</sub>F<sub>13</sub>), shows a highly water repellent surface with good film-forming properties. The characterization of the surface and cross-section of the DAP coating as well as the release rates of N and P nutrients were investigated. The following conclusions can be drawn: (i) there is good adhesion between the granules and the coating films; (ii) the total N and P nutrient release time of the coated DAP could be controlled by adjusting the thickness of the PTFEMA and PPFEHEMA coatings (1L and 2L); (iii) compared to uncoated DAP granules, which are totally solubilized after less than 2 h, coated DAP with 2L of PPFEHEMA shows the slowest N and P nutrient releases, and the P release profile of the granules coated with

PPFEHEMA 2L reached the equilibrium stage after approximately 50.5 h. The applied strategy is a promising technology allowed the very slow release and long-term availability of nutrient sources with highly hydrophobic coatings. Therefore, the proposed SFR coatings exhibit promising applications for the development of modern agriculture by improving nutrient uptake by plants, minimizing nutrient losses, and reducing environmental pollution.

The kinetic release of N and P nutrients in the soil and agronomic studies are under investigation.

## Author contributions

Asma Sofyane: methodology, investigation, writing – original draft. Salima Atlas: visualization, formal analysis, writing – review, and editing. Mohammed Lahcini: formal analysis, review, and editing. Elvira Vidović: validation, review, and editing. Bruno Ameduri: visualization, formal analysis, validation. Mustapha Raihane: conceptualization, methodology, supervision, project administration, funding acquisition, validation, writing – review, and editing. All authors have read and agreed to the published version of the manuscript.

## Data availability

Industries of commercially available coated fertilizers by polymers, mathematical modelling of release kinetics, FTIR spectra of TFEMA, PTFEMA, PFEHEMA and PPFEHEMA; water contact angle (WCA) of: (a) PTFEMA and (b) PPFEHEMA; elastic behavior of PPFEHEMA after stretching; thickness of DAP coated with PTFEMA and PPFEHEMA 1L and 2L and the corresponding coating weight percentage % (red color); nutrient saturation time of uncoated DAP and coated DAP using PTFEMA and PPFEHEMA 1L and 2L; example of release kinetic plots  $\ln(M_t/M_\infty)$  *versus*  $\ln(t)$  of coated DAP with PTFEMA and PPFEHEMA. All the data have been supplied in the ESI.†

Data provided in the manuscript are directly associated with the article.





## Conflicts of interest

There are no conflicts to declare.

## Acknowledgements

The authors would like to thank to the support through the R&D Initiative – Call project APPHOS (project ID: VAL-RAI-01/2017) for supporting this work. We also thank the Erasmus<sup>+</sup> program between Cadi-Ayyad University of Marrakech (Morocco) and Zagreb University (Croatia), and the Center of Analysis and Characterization of Cadi Ayyad University (CAC-CAU). Tosoh Finechemical Corp, Yamaguchi (Japan) is also acknowledged for the free gift of 2,2,2-trifluoroethyl methacrylate (TFEMA).

## References

- N. Alexandratos and J. Bruinsma, *WORLD AGRICULTURE TOWARDS 2030/2050 The 2012 Revision*, Food Agric. Organ. United Nations, 2012, (no. 12), p. 146, DOI: [10.1016/S0264-8377\(03\)00047-4](https://doi.org/10.1016/S0264-8377(03)00047-4).
- K. Pawlak and M. Kołodziejczak, *Sustainability*, 2020, **12**, 5488.
- C. M. Nascimento, W. de Sousa Mendes, N. E. Quiñonez Silvero, R. R. Poppiel, V. M. Sayão, A. C. Dotto, N. Valadares dos Santos, M. T. Accorsi Amorim and J. A. M. Demattê, *J. Environ. Manage.*, 2021, **277**, 111316.
- M. C. DeRosa, C. Monreal, M. Schnitzer, R. Walsh and Y. Sultan, *Nat. Nanotechnol.*, 2010, **5**, 91–91.
- Z. Chen, T. Liu, J. Dong, G. Chen, Z. Li, J. Zhou and Z. Chen, *ACS Sustainable Chem. Eng.*, 2023, **11**, 1–12.
- S. Sair, S. Aboulhrouz, O. Amadine, I. Ayouch, I. Jioui, Y. Essamlali, K. Danoun, B. Ouadil and M. Zahouily, *Eur. Polym. J.*, 2023, **199**, 112477.
- Y. Shang, Md. K. Hasan, G. J. Ahammed, M. Li, H. Yin and J. Zhou, *Molecules*, 2019, **24**, 2558.
- I. Ganetri, Y. Essamlali, O. Amadine, K. Danoun, S. Aboulhrouz and M. Zahouily, *Controlling factors of slow or controlled-release fertilizers*, Elsevier Inc., 2021.
- T. El Assimi, O. Lakbita, A. El Meziane, M. Khouloud, A. Dahchour, R. Beniazza, R. Boulif, M. Raihane and M. Lahcini, *Int. J. Biol. Macromol.*, 2020, **161**, 492–502.
- M. E. Trenkel, *Slow- and Controlled Release and Stabilized Fertilizers in Agriculture. An Option for Enhancing Nutrient Use Efficiency in Agriculture*, International Fertilizer Industry Association (IFA), Paris, 2nd edn, 2010.
- S. M. Al-Zahrani, *Ind. Eng. Chem. Res.*, 2000, **39**, 367–371.
- A. Jarosiewicz and M. Tomaszewska, *J. Agric. Food Chem.*, 2003, **51**, 413–417.
- A. Olad, M. Pourkhiyabi, H. Gharekhani and F. Doustdar, *Carbohydr. Polym.*, 2018, **190**, 295–306.
- A. Rashidzadeh and A. Olad, *Carbohydr. Polym.*, 2014, **114**, 269–278.
- Z. Zhou, Y. Shen, C. Du, J. Zhou, Y. Qin and Y. Wu, *Land Degrad. Dev.*, 2017, **28**, 2370–2379.
- E. L. Krasnopeeva, G. G. Panova and A. V. Yakimansky, *Int. J. Mol. Sci.*, 2022, **23**, 15134.
- S. Qian, F. Zhang, B. Liu, H. Ren and G. Tong, *BioResources*, 2017, **12**(3), 6607–6617.
- T. G. Liu, Y. T. Wang, J. Guo, T. B. Liu, X. Wang and B. Li, *J. Appl. Polym. Sci.*, 2017, **134**, 45175.
- J. Zhu, W. K. Tan, X. Song, Z. Zhang, Z. Gao, Y. Wen, C. N. Ong, S. Swarup and J. Li, *ACS Food Sci. Technol.*, 2023, **3**, 553–561.
- P. Jumpapaeng, P. Suwanakood, S. Nanan and S. Saengsuwan, *J. Ind. Eng. Chem.*, 2023, **127**, 191–209.
- W. Yao, Y. Li and X. Huang, *Polymer*, 2014, **55**, 6197–6211.
- D. W. Smith, S. T. Iacono and S. S. Iyer, *Handbook of Fluoropolymer Science and Technology*, New York, 2014.
- B. Ameduri and H. Sawada, *Fluorinated Polymers Applications*, Cambridge, UK, 2017th edn, 2017, vol. 2.
- R. Ishige, T. Shinohara, K. L. White, A. Meskini, M. Raihane, A. Takahara and B. Ameduri, *Macromolecules*, 2014, **47**, 3860–3870.
- G. Alessandrini, M. Aglietto, V. Castelvetro, F. Ciardelli, R. Peruzzi and L. Toniolo, *J. Appl. Polym. Sci.*, 2000, **76**, 962–977.
- I. Yamamoto, in *Fluorinated Polymers: Volume 2: Applications*, ed. B. Ameduri, H. Sawada, B. Ameduri and H. Sawada, The Royal Society of Chemistry, 2016, vol. 2.
- V. Castelvetro, M. Aglietto, F. Ciardelli, O. Chiantore, M. Lazzari and L. Toniolo, *J. Coat. Technol.*, 2002, **74**, 57–66.
- V. Sabatini, E. Pargoletti, V. Comite, M. A. Ortenzi, P. Fermo, D. Gulotta and G. Cappelletti, *Polymers*, 2019, **11**, 1190.
- Z. Gu, M. Zhang, J. He and P. Ni, *Colloids Surf., A*, 2016, **502**, 159–167.
- S. Chen, Y. Han, M. Yang, X. Zhu, C. Liu, H. Liu and H. Zou, *Prog. Org. Coat.*, 2020, **149**, 105964.
- A. Sofyane, E. Ben Ayed, M. Lahcini, M. Khouloud, H. Kaddami, B. Ameduri, S. Boufi and M. Raihane, *Eur. Polym. J.*, 2021, **156**, 110598.
- M. Stone, T. G. Nevell and J. Tsibouklis, *Mater. Lett.*, 1998, **37**, 102–105.
- B. Ameduri, J. Sales and M. Schlipf, *Int. Chem. Regul. Law Rev.*, 2023, **6**, 18–28.
- T. Shirai, H. Fukumoto, Y. Kanno, T. Kubota and T. Agou, *Polymer*, 2021, **217**, 123478.
- V. Kumar, J. Pulpytel and F. Arefi-Khonsari, *Plasma Processes Polym.*, 2010, **7**, 939–950.
- Q. Zhang, Q. Wang, J. Jiang, X. Zhan and F. Chen, *Langmuir*, 2015, **31**, 4752–4760.
- A. Kadimi, H. Kaddami, Z. Ounaies, Y. Habibi, R. Dieden, B. Ameduri and M. Raihane, *Polym. Chem.*, 2019, **10**, 5507–5521.
- M. Raihane and B. Ameduri, *J. Fluorine Chem.*, 2006, **127**, 391–399.
- Y. Liu, Y. Higaki, M. Mukai and A. Takahara, *Polymer*, 2019, **182**, 121846.



- 40 A. Sofyane, E. Ablouh, M. Lahcini, A. Elmeziane, M. Khoulood, H. Kaddami and M. Raihane, *Mater. Today: Proc.*, 2021, **36**, 74–81.
- 41 E. Barbu, R. A. Pullin, P. Graham, P. Eaton, R. J. Ewen, J. D. Smart, T. G. Nevell and J. Tsibouklis, *Polymer*, 2002, **43**, 1727–1734.
- 42 J. Tsibouklis, P. Graham, P. J. Eaton, J. R. Smith, T. G. Nevell, J. D. Smart and R. J. Ewen, *Macromolecules*, 2000, **33**, 8460–8465.
- 43 Y. Xu, W. Wang, Y. Wang, J. Zhu, D. Uhrig, X. Lu, J. K. Keum, J. W. Mays and K. Hong, *Polym. Chem.*, 2016, **7**, 680–688.
- 44 R. W. Phillips and R. H. Dettre, *J. Colloid Interface Sci.*, 1976, **56**, 251–254.
- 45 M. Karamane, M. Raihane, M. A. Tasdelen, T. Uyar, M. Lahcini, M. Ilsouk and Y. Yagci, *J. Polym. Sci., Part A: Polym. Chem.*, 2017, **55**, 411–418.
- 46 V. Castelvetro, M. Raihane, S. Bianchi, S. Atlas and I. Bonaduce, *Polym. Degrad. Stab.*, 2011, **96**, 204–211.
- 47 B. Ameduri, *Well Architected Fluoropolymers: Synthesis, Properties and Applications*, Elsevier, Amsterdam, 2004.
- 48 A. Sofyane, M. Lahcini, A. El Meziane, M. Khoulood, A. Dahchour, S. Caillol and M. Raihane, *J. Am. Oil Chem. Soc.*, 2020, **97**, 751–763.
- 49 E. H. Boutrouia, T. El Assimi, M. Raihane, R. Beniazza, H. Ben Youcef, M. Khoulood, M. H. V. Baouab, A. El Kadib and M. Lahcini, *Prog. Org. Coat.*, 2022, **172**, 107102.
- 50 M. Devassine, F. Henry, P. Guerin and X. Briand, *Int. J. Pharm.*, 2002, **242**, 399–404.
- 51 S. K. Yadavalli, M. Chen, M. Hu, Z. Dai, Y. Zhou and N. P. Padture, *Scr. Mater.*, 2020, **187**, 88–92.
- 52 T. Li, S. Lü, Y. Ji, T. Qi and M. Liu, *New J. Chem.*, 2018, **42**, 19129–19136.
- 53 E. I. Pereira, F. B. Minussi, C. C. T. da Cruz, A. C. C. Bernardi and C. Ribeiro, *J. Agric. Food Chem.*, 2012, **60**, 5267–5272.
- 54 D. F. da Cruz, R. Bortoletto-Santos, G. G. F. Guimarães, W. L. Polito and C. Ribeiro, *J. Agric. Food Chem.*, 2017, **65**, 5890–5895.
- 55 P. L. Ritger and N. A. Peppas, *J. Controlled Release*, 1987, **5**, 23–36.

